

Environmental scanning electron microscopy (ESEM) as a new technique to determine the ice nucleation capability of individual atmospheric aerosol particles

Frank Zimmermann^{a,*}, Martin Ebert^a, Annette Worringen^a,
Lothar Schütz^b, Stephan Weinbruch^a

^a*Institute of Applied Geosciences, Technical University Darmstadt, Schnittspahnstr. 9, 64287 Darmstadt, Germany*

^b*Institute for Atmospheric Physics, Johannes-Gutenberg University, Johann-Joachim-Becher-Weg 21, 55099 Mainz, Germany*

Received 18 December 2006; received in revised form 14 June 2007; accepted 21 June 2007

Abstract

Heterogeneous ice nucleation on synthetic silver iodide, natural kaolinite and montmorillonite particles via condensation, freezing and deposition modes was studied by environmental scanning electron microscopy (ESEM) in the temperature range of 250–270 K. By increasing the H₂O pressure in the sample chamber at constant temperature, ice formation can be studied in situ and can be related to the chemical composition of the particles that can be determined simultaneously. For silver iodide and kaolinite, supersaturation values of first ice formation are in good agreement (1–2% absolute) with diffusion chamber experiments. For both substances, threshold temperatures for the condensation, freezing and deposition modes are also in good agreement (within 2 K) with previous literature data. For montmorillonite, ESEM results for the supersaturation value of first ice formation and for threshold temperatures of condensation freezing and deposition mode lie within the large range reported in the literature.

© 2007 Elsevier Ltd. All rights reserved.

Keywords: Environmental scanning electron microscopy; Ice nucleation; Deposition freezing; Condensation freezing

1. Introduction

Ice nucleation occurs in the atmosphere in two primary ways: by homogeneous freezing of liquid solution droplets and by heterogeneous interaction with a particulate nucleus (e.g., Vali, 1985; Pruppacher and Klett, 1997). Heterogeneous freezing is initiated by the presence of solid particles with an

appropriate structure, the so called “ice nuclei” (IN) (e.g., Roddy and O’Connor, 1981). For both processes, nucleation efficiency varies with temperature and supersaturation with respect to ice. Only a small fraction of atmospheric aerosol particles (AP) act as IN, and the IN/AP ratio varies between 10⁻³ and 10⁻⁶ (e.g., Pruppacher and Klett, 1997). Ice nuclei act in four different modes: deposition, contact freezing, immersion freezing and condensation freezing (Vali, 1985; Pruppacher and Klett, 1997). All four nucleation modes may occur in the atmosphere. However, for ice cloud formation the exact fraction of each mode is not known.

*Corresponding author. Tel.: +49 6151 1643 44;
fax: +49 6151 1640 21.

E-mail address: zimmer_f@geo.tu-darmstadt.de
(F. Zimmermann).

Modelling studies have shown that the type and quantity of atmospheric aerosol particles acting as ice nuclei can influence ice cloud microphysical and radiative properties as well as their precipitation efficiency (e.g., Jensen et al., 2001; Gierens, 2003; Haag and Kärcher, 2004). Therefore, a quantitative description of the ice nucleation processes is crucial for a better understanding of formation, life cycles and the optical properties of clouds.

Ice nucleation was studied in a large number of laboratory and field experiments (for reviews, see Mossop, 1963; Pruppacher and Klett, 1997; DeMott, 2002). A variety of measurement techniques was developed for this purpose: rapid expansion cloud chamber (Bigg, 1957), mixing chamber (Langer, 1973), continuous flow diffusion chamber (Rogers, 1988), aerosol collection on membrane filters followed by processing in a diffusion chamber (Bigg, 1990) and slow expansion cloud chamber to simulate realistic updrafts (Rogers et al., 1996). All these measurements are based on exposing aerosols to a cold supersaturated environment and counting the ice crystals that nucleate and grow to detectable size.

Environmental scanning electron microscopy (ESEM) enables *in situ* observation of interactions between water vapour and aerosol particles in the sub-micrometre range (e.g., Ebert et al., 2002; Hoffman et al., 2004). By varying the water partial pressure and using a Peltier element to realise temperatures below the freezing point, it is possible to obtain supersaturated conditions relative to ice in the sample chamber of an environmental scanning electron microscope. Thus, ice formation and ice crystal growth can be imaged with this technique. It is not possible to study the nucleation process itself, due to the lateral resolution of the instrument which is limited to approximately 20 nm. However, it can be concluded that ice nucleation occurred at the same location (i.e., on the same aerosol particle), where ice crystal growth is observed.

In addition, the chemical composition of individual particles can be studied simultaneously by energy-dispersive X-ray (EDX) microanalysis. Another advantage of ESEM is that insulating samples need no conductive coating for charge compensation. Therefore, aerosol particles and their ice nucleation ability can be investigated without any sample preparation and the surface morphology is not obscured by the coating. Hence, it is possible to relate the ice formation behaviour of individual particles to their chemical composition and mixing

state, which is a great advantage for the study of ambient aerosol samples.

In the present paper, we want to demonstrate that the ice nucleation capability of individual aerosol particles can be determined accurately by ESEM. For this purpose, particles of synthetic silver iodide and of minerals (kaolinite, montmorillonite) with known ice nucleation behaviour and well-documented threshold temperatures for the deposition and condensation freezing modes of nucleation are investigated. We are currently extending our ESEM investigations to real atmospheric particles in order to relate the ice forming properties to the chemical composition and mixing state (e.g., external vs. internal mixture, surface coatings) of the particles.

2. Experimental

2.1. Instrumentation

A first set of measurements was carried out in a PHILIPS XL30 ESEM LaB₆ instrument, but most investigations were performed with a FEI Quanta 200 FEG instrument. Both electron microscopes are equipped with an EDX detector for microanalysis. The special design of the vacuum system of both instruments allows working pressures up to approximately 40 hPa in the sample chamber during imaging with secondary and backscattered electrons. Details of ESEM can be found elsewhere (e.g., Danilatos, 1988; Goldstein et al., 2003). The working pressure can be set by any non-flammable and non-corrosive gas including H₂O. In our experiments, the total pressure in the sample chamber was always equal to the partial pressure of H₂O, i.e., no other gas species was present inside the sample chamber. The pressure in the sample chamber was varied in steps of ≈ 0.13 hPa with the Philips XL30 ESEM LaB₆ and in steps of 0.1 hPa with the FEI Quanta 200 FEG. These steps in pressure regulation are equivalent to a change in the supersaturation on the order of 2% at a temperature of 273 K, and about 12% at lower temperatures around 250 K. Therefore, precise determination of ice activation by ESEM is restricted (at least with current instrumentation) to temperatures above ≈ 250 K. In this context, it should be noted that the FEI Quanta 200 FEG nominally allows pressure regulation in finer steps of 0.01 hPa. However, these small steps are not suitable for activation experiments, as it turned out during our work that this fine regulation in 0.01 hPa steps is not accurate. In

addition, the pressure stability of the instrument is <0.01 hPa. We also experienced systematic shifts in the pressure reading on the order of 0.2 hPa in both instruments, which occurred on a time scale of several months. Therefore, it is necessary to calibrate the sample chamber pressure, at least on a weekly basis (see chapter 2.3.), or to measure the pressure independently from the instrumental reading. We are currently using an additional pressure transducer (Setra, Vactron, model 760) to obtain accurate results for the sample chamber pressure. The sample temperature can be varied in steps of 0.1 K with a Peltier element (FEI, FP 6750). The Peltier element was cooled with a glycol–water mixture as a cooling agent. To minimize thermal gradients, a small specimen stub made of copper (Fig. 1) was used in the ice nucleation experiments.

2.2. Particle preparation

Particles of silver iodide (AgI) were prepared from p.a. grade substances by grinding. For kaolinite $\text{Al}_4[\text{Si}_4\text{O}_{10}](\text{OH})_8$, and montmorillonite $(\text{Ca},\text{Na})_x(\text{Al},\text{Mg},\text{Fe})_2[\text{Si}_4\text{O}_{10}](\text{OH})_2 \cdot n\text{H}_2\text{O}$, phases commonly found in mineral dust samples (e.g., Glacuum and Prospero, 1980), standards distributed by The Clay Minerals Society (CMS Chipera and Bish, 2001) were used in our experiments.

Particle diameter varied mostly between 1 and $10\ \mu\text{m}$, few particles were larger with diameters up to $100\ \mu\text{m}$. However, ice nucleation only occurred on particles $<10\ \mu\text{m}$. Phase composition of the standard materials was checked by X-ray powder diffraction analysis. The particles were spread on a silicon plate ($5 \times 5\ \text{mm}$), which was placed into a self-constructed silanized (2% solution of dichlorodimethylsilan in 1,1,1 trichlorethan) Cu-adapter (Fig. 1). The silanization yields a hydrophobic surface by forming a monolayer of silanes which suppresses ice formation on the copper surface. The silanization procedure has to be repeated after every third measurement cycle. A thin layer of a silicon-free heat conductor paste (GLT, Pforzheim, Germany) was applied between the Cu adapter and the Peltier element.

2.3. Calibration

Prior to the ice nucleation experiments, the temperature of the Peltier element was calibrated by determination of the deliquescence relative humidity (DRH) of different salts (Ebert et al., 2002). During these calibration experiments, the temperature was measured at the surface of the Cu adapter with a resistance temperature sensor (Pt 1000). For all salt particles investigated (NaCl,

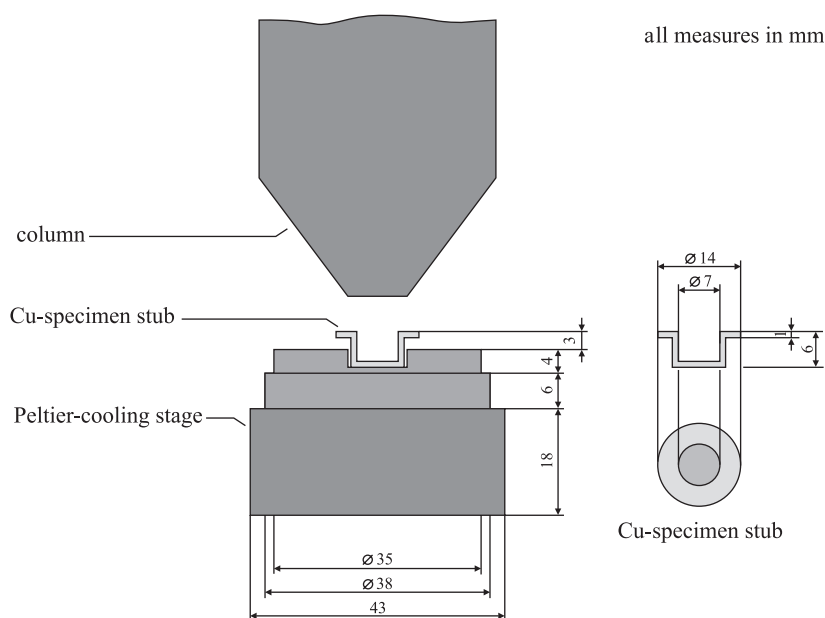


Fig. 1. Detailed schematic of the Cu-specimen stub used for ice nucleation experiments.

NH_4NO_3 , Na_2SO_4), the literature data for the DRH and its temperature dependence were reproduced within error limits (for details, see Ebert et al., 2002) demonstrating that temperature and total pressure (which is identical with the H_2O partial pressure) were determined accurately.

2.4. Ice nucleation experiments

The ice nucleation behaviour of the different particles was studied by the following procedure. After the particles were placed on the substrate, the sample chamber was evacuated to remove any ambient gases in the system. The temperature of the external water cooler was set to 258 K and the cooling stage was cooled down to temperatures slightly above the freezing point of water. After turning on the electron beam and focusing, the Peltier element was switched on. In each experimental session, the ice nucleation ability was investigated for one substance at different temperatures, starting with the highest temperature of the investigated range. The appropriate starting temperature was determined by preliminary experiments and was set to 264 K, except for AgI, where the starting temperature was 270 K. The temperature was then reduced stepwise by 1 K down to 250 K. For each temperature, the H_2O partial pressure (total sample chamber pressure) was increased in steps of 0.13 hPa (Philips XL30 ESEM LaB₆) or 0.1 hPa (FEI Quanta 200 FEG) starting at 0.5 hPa. After each pressure increase, the sample was inspected for 5–10 min before the pressure was raised again. The partial pressure of H_2O was increased until ice formation was observed on the particles (two typical examples are given in Fig. 2). Crystallization of ice leads to the liberation of latent heat, and a slight increase in the temperature can be registered at the Peltier element. The H_2O partial pressure at this point was taken to calculate the supersaturation over ice. The saturation vapour pressures with respect to water (p_{sw}) and ice (p_{si}) are taken from Buck (1981)

$$p_{\text{sw}}[\text{hPa}] = 6.1121 \exp(17.9662(T[^\circ\text{C}]/(T[^\circ\text{C}] + 247.15))), \quad (1)$$

$$p_{\text{si}}[\text{hPa}] = 6.1115 \exp(22.452(T[^\circ\text{C}]/(T[^\circ\text{C}] + 272.55))). \quad (2)$$

After ice formation was observed, the pressure was reduced again in steps of ≈ 0.1 hPa, down to the

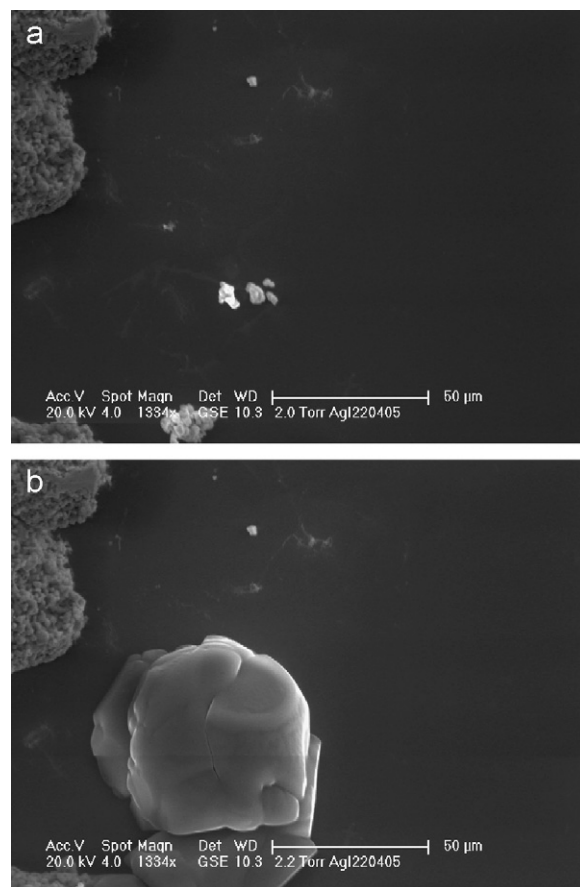


Fig. 2. Secondary electron images of ice formation on individual aerosol particles. (a) before ice nucleation (b) after onset of ice nucleation.

point where all the ice was evaporated (Fig. 2). Then the pressure cycle was repeated twice (at constant temperature).

All experiments were carried out at magnifications approximately $< 1000 \times$. Higher magnification (i.e., higher current densities), which would be favourable for the detection of small morphological details, led to melting or evaporation of the ice crystals. Melting or evaporation of ice at high magnifications is most likely caused by a temperature rise induced by the electron beam. At magnifications $\leq 1000 \times$, ice crystals were stable during all investigations. In selected cases, the secondary electron signal was stored as a digital video file during the whole experiment (one example is given as Supplementary data).

In order to check that ice nucleation is initiated by the particles, an experiment with a pure substrate (i.e., without particles) was performed. In this case,

ice formation was not observed, even at high supersaturation values up to approximately 140% (relative to ice).

For heterogeneous reactions between gas phase hydroxyl radicals and liquid droplets of deliquesced sodium chloride particles, it was shown recently by Laskin et al. (2006) that the particle surface density may influence the water vapour pressure above the particles. This process would lead to an over-estimation of the supersaturation. However, with the particle concentrations on the substrate used in the present paper (100–150 particles mm^{-2}) such an effect was not observed. This is in good agreement with the results of Laskin et al. (2006), who also did not observe an influence of the particle surface density at a similar particle concentration. Only much higher particle concentrations led to measurable effects on ice nucleation. In addition, the good agreement of our results with previous work also suggests that the effect of particle surface density can be neglected.

3. Results and discussion

We have determined the supersaturation value where ice formation is first observed as function of temperature. In addition, the threshold temperatures for ice formation by the condensation freezing and deposition freezing modes were derived.

A few important general observations are summarized in the following, before the results for the different materials are discussed separately:

- (a) In all experiments, ice nucleation was induced only by a small number of particles. The exact fraction of particles activated cannot be determined precisely, as only a small part of the substrate is imaged with the used magnifications.
- (b) With decreasing temperature (increasing supersaturation) the number of activated particles increases.
- (c) The rate of crystal growth increases with decreasing temperature and increasing supersaturation.
- (d) In some cases, activation of a particle is not reproducible, i.e., a particle that acted as an ice nucleus cannot be activated in further cycles. A similar behaviour was observed by Soulage (1957) for natural mineral dust particles.

3.1. Silver iodide

The ESEM results for ice formation in the deposition and condensation freezing modes obtained with both different instruments (PHILIPS XL 30 ESEM LaB₆ and FEI Quanta 200 FEG) are shown in Fig. 3. For comparison, data from diffusion chamber experiments of Schaller and Fukuta (1979) are also displayed. Data points of the Schaller and Fukuta (1979) experiments represent 1.3% of ice nucleation within 1 min. Supersaturation values obtained with the FEI Quanta 200 FEG are generally 1–2% lower than those received with the PHILIPS XL 30 ESEM LaB₆. This difference can be easily explained by the fact that the pressure can be regulated in finer steps with the FEI instrument (0.10 hPa vs. 0.13 hPa) allowing a more accurate determination of the onset of ice formation. Supersaturation values obtained with the FEI Quanta 200 FEG instrument are in good agreement with the results for 1.3% of ice nucleation within 1 min reported by Schaller and Fukuta (1979), while findings of the Philips XL 30 ESEM fit well with the results for 3.2% ice nucleation (not shown in Fig. 3) determined by the same authors. However, estimation of the exact extent of ice nucleation is not possible in our investigations, because crystal growth of ice is very fast in an atmosphere consisting of pure water vapour. Within 1 min, almost the complete substrate surface will be iced. Therefore, the slight increase in temperature recorded by the Peltier element (caused by release of latent heat) was used to determine the onset of ice formation and the corresponding supersaturation value (see above). The threshold temperatures for ice formation (Table 1) were determined from supersaturation vs. temperature plots (Figs. 3–5) for the condensation freezing (T_c) and deposition mode (T_d). For silver iodide, first ice formation in the condensation freezing mode was observed at a temperature of 268 K, and in the deposition mode at a temperature of 264 K (Fig. 3). These threshold temperatures determined by ESEM are in good agreement with earlier work carried out with diffusion chambers (Table 1).

3.2. Kaolinite

The ESEM results for kaolinite are displayed in Fig. 4 together with the findings of previous experiments (Schaller and Fukuta, 1979; Bailey

Table 1

Comparison of the threshold temperatures of ice formation for condensation freezing mode and deposition mode

Condensation freezing mode			
AgI	Kaolinite	Montmorillonite	Reference ^a
268	263	259.5	This work
268.5	263.1	n.d.	1
n.d.	262.5	248	2
269	n.d.	n.d.	3
Deposition mode			
264	254	248	This work
264.3	254	n.d.	1
n.d.	254	< 246	2
261	n.d.	n.d.	3
n.d.	261	n.d.	4
n.d.	251	258	5

^a1: Schaller and Fukuta (1979); 2: Roberts and Hallett (1968); 3: Bryant et al. (1959); 4: Bailey and Hallett (2002); 5: Salam et al. (2006); n.d. = not determined.

and Hallett, 2002; Salam et al., 2006; Dymarska et al., 2006). The difference between the two electron microscopes is less pronounced compared with silver iodide (the difference is smaller than the data points in Fig. 4). As can be seen from Fig. 4, supersaturation values for the onset of ice formation determined by ESEM are in good agreement with the diffusion chamber experiments of Schaller and Fukuta (1979), which represent 1.3% ice nucleation within 1 min, as well as with the results of Dymarska et al. (2006). The threshold temperatures obtained from ESEM for condensation freezing (263 K) and for deposition (254 K) modes, in general agree well with previous diffusion chamber experiments, except for the work of Bailey and Hallett (2002).

According to Roberts and Hallett (1968), kaolinite grains can be preactivated, i.e., in a second cooling cycle ice formation occurred at more grains or at higher temperatures compared with the initial

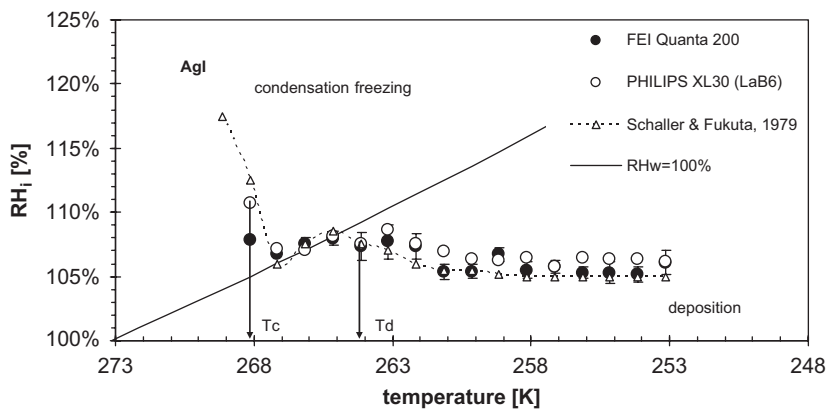


Fig. 3. Supersaturation vs. temperature diagram for silver iodide.

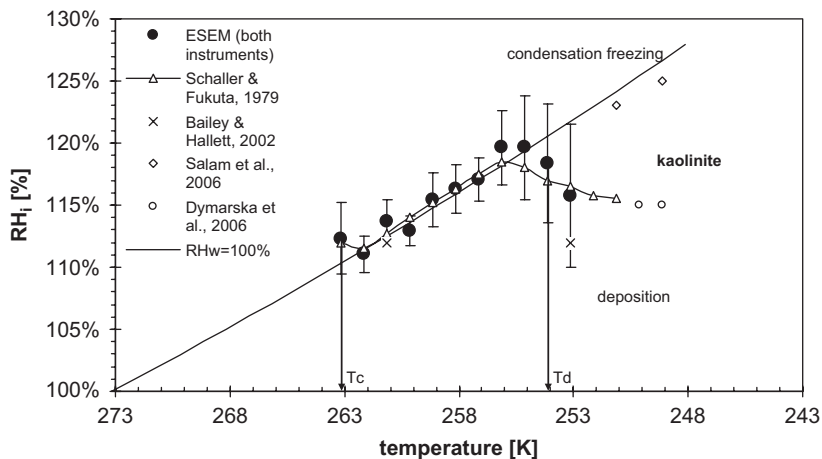


Fig. 4. Supersaturation vs. temperature diagram for kaolinite.

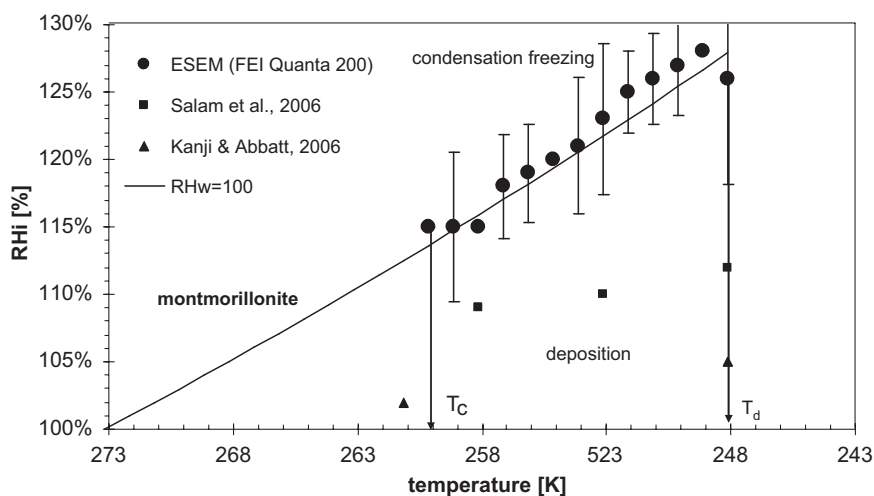


Fig. 5. Supersaturation vs. temperature diagram for montmorillonite.

cooling step. Such behaviour was not observed in our experiments.

3.3. Montmorillonite

Experimental results for montmorillonite in literature are contradictory (Fig. 5 and Table 1). In our work, ice nucleation in the deposition mode was not observed at temperatures above 252 K. This is in general agreement with the results of former investigations with a diffusion chamber (Roberts and Hallett, 1968), who reported a critical temperature of 246 K for ice nucleation via the deposition mode. In contrast, ice nucleation was observed in the deposition mode at temperatures between 258 and 261 K by Salam et al. (2006) and Kanji and Abbatt (2006). According to Salam et al. (2006) ice formation in the deposition mode occurs at a relative humidities (RH_i) with respect to ice at around 110%, whereas Kanji and Abbatt (2006) observed the onset of ice formation at much lower RH_i, that is between 102 and 105% (Fig. 5). Kanji and Abbatt discussed three possibilities to explain the observed discrepancy: (i) a time effect due to the longer duration of their experiments compared with Roberts and Hallett (1968), (ii) a preactivation effect and (iii) a preparation effect.

For condensation freezing, Roberts and Hallett (1968) found no ice formation above 248 K. In contrast, we observed ice nucleation via condensation freezing at 260 K at a RH_i of 114% (Fig. 5). However, Roberts and Hallett (1968) reported a critical temperature of 259.5 K and a minimum ice

supersaturation of 14% when the particles were preactivated.

The threshold temperatures for deposition and condensation mode nucleation (Table 1) are also conflicting. The threshold temperature T_d for deposition mode ice formation obtained from ESEM is in good agreement with the observations of Roberts and Hallett (1968), but is much lower compared with recent work (Salam et al., 2006; Kanji and Abbatt, 2006). For the condensation mode, threshold temperatures from ESEM are higher than those reported by Roberts and Hallett (1968), but are in agreement with earlier experiments (Mason and Maybank, 1958: 255 K for 100 ice crystals per 10^6 particles; Mason, 1960: 257 K for 100 ice crystals per 10^6 particles; Hoffer, 1961: 259.5 K; Pitter and Pruppacher, 1973: 259 K). Hoffer (1961) also reported a large range of freezing temperatures for montmorillonite, from 259.5 to 237.5 K. As already noted by Hoffer (1961), the large variation in the chemical composition of montmorillonite may be responsible for the observed variation in condensation mode threshold temperatures.

4. Conclusions

1. Heterogeneous ice nucleation on individual aerosol particles can be studied quantitatively by ESEM. By increasing the H₂O vapour pressure at constant temperature, the condensation freezing and deposition modes can be investigated. These freezing experiments can also

be done with ambient samples in ESEM (equipped with EDX), which will then allow the chemical identification of the ambient ice nuclei.

- For silver iodide and kaolinite, supersaturation values of first ice formation (at constant temperature) obtained by ESEM generally agree within 1–2% (absolute) with previous work in diffusion chambers. Threshold temperatures for condensation freezing and deposition mode determined by ESEM are also in good agreement (generally within 2K) with diffusion chamber experiments.
- For montmorillonite, literature data for supersaturation values of first ice formation and for threshold temperatures are quite variable. The results of ESEM lie within the range reported in previous studies.

Acknowledgments

We thank H. Hoffmann (University Darmstadt) for X-ray powder diffraction analysis of kaolinite and montmorillonite standard samples, and S. Mitra and K. Diehl (University of Mainz) for helpful discussions. Financial support by the German Science Foundation (Sonderforschungsbereich 641 “The tropospheric ice phase”) is gratefully acknowledged.

Appendix A. Supplementary data

The online version of this article contains additional supplementary data. Please visit [doi:10.1016/j.atmosenv.2007.06.023](https://doi.org/10.1016/j.atmosenv.2007.06.023).

References

- Bailey, M., Hallett, J., 2002. Nucleation effects on the habit of vapour grown ice crystals from -18 to 42°C . *Quarterly Journal of the Royal Meteorological Society* 128, 1461–1468.
- Bigg, E.K., 1957. A new technique for counting ice-forming nuclei in aerosols. *Tellus* 9, 394–400.
- Bigg, E.K., 1990. Measurement of concentrations of natural ice nuclei. *Atmospheric Research* 25, 397–408.
- Bryant, G.W., Hallett, J., Mason, B.J., 1959. The epitaxial growth of ice on single crystalline substrates. *Journal of Physics and Chemistry of Solids* 12, 189–195.
- Buck, A.L., 1981. New equations for computing vapor pressure and enhancement factor. *Journal of Applied Meteorology* 20, 1527–1532.
- Chopera, S.J., Bish, D.L., 2001. Baseline studies of The Clay Minerals Society source clays: powder X-ray diffraction analyses. *Clays and Clay Minerals* 49, 398–409.
- Danilatos, G.D., 1988. Foundations of environmental scanning electron microscopy. *Advances in Electronics and Electron Physics* 71, 109–205.
- DeMott, P.J., 2002. Laboratory studies of cirrus cloud processes. In: Lynch, D.K. (Ed.), *Cirrus*. Oxford University Press, New York, pp. 102–135 (Chapter 5).
- Dymarska, M., Murray, B.J., Sun, L., Eastwood, M.L., Knopf, D.A., Bertram, A.K., 2006. Deposition ice nucleation on soot at temperatures relevant for the lower troposphere. *Journal of Geophysical Research* 111, D04204.
- Ebert, M., Inerle-Hof, M., Weinbruch, S., 2002. Environmental scanning electron microscopy as a new technique to determine the hygroscopic behaviour of individual aerosol particles. *Atmospheric Environment* 36, 5909–5916.
- Gierens, K., 2003. On the transition between heterogeneous and homogeneous freezing. *Atmospheric Chemistry and Physics* 3, 437–446.
- Glacuum, R.A., Prospero, J.M., 1980. Saharan aerosols over the tropical North Atlantic–Mineralogy. *Maritime Geology* 37, 295–321.
- Goldstein, J.I., Newbury, D.E., Joy, D.C., Lyman, C.E., Echlin, P., Lifshin, E., Sawyer, L., Michael, J.R., 2003. *Scanning Electron Microscopy and X-ray Microanalysis*, third ed. Springer, New York.
- Haag, W., Kärcher, B., 2004. The impact of aerosols and gravity waves on cirrus clouds at mid-latitudes. *Journal of Geophysical Research* 109, D12202, doi:10.1029/2004JD004579.
- Hoffer, T., 1961. A laboratory investigation of droplet freezing. *Journal of Meteorology* 18, 766–778.
- Hoffman, R.C., Laskin, A., Finlayson-Pitts, B.J., 2004. Sodium nitrate particles: physical and chemical properties during hydration and dehydration, and implications for aged sea salt aerosols. *Journal of Aerosol Science* 35, 869–887.
- Jensen, E.J., Toon, O.B., Vay, S.A., Ovarlez, J., May, R., Bui, P., Twohy, C.H., Gandrud, B.W., Poeschel, R.F., Schumann, U., 2001. Prevalence of ice supersaturated regions in the upper troposphere: implications for optically thin ice cloud formation. *Journal of Geophysical Research* 106, 17253–17266.
- Kanji, Z.A., Abbatt, J.P.D., 2006. Laboratory studies of ice formation via deposition mode nucleation onto mineral dust and n-hexane soot samples. *Journal of Geophysical Research* 111, D16204.
- Langer, G., 1973. Evaluation of NCAR ice nucleus counter. Part I: basic operation. *Journal of Applied Meteorology* 12, 1000–1011.
- Laskin, A., Wang, H., Robertson, W.H., Cowin, J.P., Ezell, M.J., Finlayson-Pitts, B.J., 2006. A new approach to determining gas-particle reaction probabilities and application to the heterogeneous reaction of deliquesced sodium chloride particles with gas-phase hydroxyl radicals. *Journal of Physical Chemistry A* 110, 10619–10627.
- Mason, B.J., 1960. Ice-nucleating properties of clay minerals and stony meteorites. *Quarterly Journal of the Royal Meteorological Society* 86, 552–556.
- Mason, B.J., Maybank, J., 1958. Ice-nucleating properties of some natural mineral dusts. *Quarterly Journal of the Royal Meteorological Society* 84, 235–241.
- Mossop, S.C., 1963. Atmospheric ice nuclei. *Zeitschrift für Angewandte Mathematik und Physik* 14, 456–486.
- Pitter, R.L., Pruppacher, H.R., 1973. A wind tunnel investigation of freezing of small water drops falling at terminal velocity in

- air. Quarterly Journal of the Royal Meteorological Society 99, 540–550.
- Pruppacher, H.R., Klett, J.D., 1997. Microphysics of Cloud and Precipitation. Kluwer, Dordrecht, 954pp.
- Roberts, P., Hallett, J., 1968. A laboratory study of the ice nucleating properties of some mineral particulates. Quarterly Journal of the Royal Meteorological Society 94, 25–34.
- Roddy, A.F., O'Connor, T.C. (Eds.), 1981. Atmospheric Aerosols and Nuclei. Galway University Press, Galway, Ireland, pp. 333–387.
- Rogers, D.C., 1988. Development of a continuous flow thermal gradient diffusion chamber for ice nucleation studies. Atmospheric Research 22, 149–181.
- Rogers, D.C., DeMott, P.J., Cooper, W.A., Rasmussen, R.M., 1996. Ice formation in wave clouds—comparison of aircraft observations with measurements of ice nuclei. In: 12th International Conference of Clouds and Precipitation, Zurich, p. 135–137.
- Salam, A., Lohmann, U., Crenna, B., Lessins, G., Klages, P., Rogers, D., Irani, R., MacGillivray, A., Coffin, M., 2006. Ice nucleation studies of mineral dust particles with a new continuous flow diffusion chamber. Aerosol Science and Technology 40, 134–141.
- Schaller, R.C., Fukuta, N., 1979. Ice nucleation by aerosol particles: Experimental studies using a wedge-shaped ice thermal diffusion chamber. Journal of Atmospheric Sciences 36, 1788–1802.
- Soulaie, G., 1957. Les noyaux de congélation de l'atmosphère. Annales de Geophysique 13, 103–134, 167–185.
- Vali, G., 1985. Nucleation terminology. Bulletin of the American Meteorological Society 66, 1426–1427.